Journal of the European Ceramic Society 21 (2001) 1775–1778

www.elsevier.com/locate/jeurceramsoc

Crystal structure, electrical and magnetic properties of perovskites $La_{0.5}Sr_{0.5-x}Ba_xCoO_3$ ($x=0.0$ and 0.25)

H.J. Kim [a,*], W.K. Choo [a], C.H. Lee [b]

[a] *Department of Materials Science and Engineering, Korea Advanced Institute of Science and Technology, 373-1 Gusong-Dong, Yusong-Gu, Taejon, South Korea*

[b] *Neutron Physics Department, Hanaro Center, Korea Atomic Energy Research Institute, Taejon, South Korea*

Received 4 September 2000; received in revised form 7 November 2000; accepted 15 November 2000

Abstract

The resistivity and magnetization of $La_{0.5}Sr_{0.5-x}Ba_xCoO_3$ ($x=0.0$ and 0.25) system have been investigated. The resistivity of $La_{0.5}Sr_{0.5-x}Ba_xCoO_3$ has increased with Ba substitution. Magnetization curves of $La_{0.5}Sr_{0.5-x}Ba_xCoO_3$ ($x=0.0$ and 0.25) have showed the large difference between field cooled M_{FC} and zero field cooled M_{ZFC} below T_c. X-ray and neutron diffraction measurements have been also performed. The crystal structure of $La_{0.5}Sr_{0.5}CoO_3$ at room temperature is rhombohedrally distorted perovskite belonging to the space group $R\bar{3}c$ (No. 167) with the $a^-a^-a^-$ type tilt system. From the results of powder X-ray and neutron Rietveld analysis, it is demonstrated that the lattice parameter along the a-axis increases and the rhombohedral angle decreases with the Ba substitution. It is also shown that the octahedral tilting becomes smaller with the Ba substitution. © 2001 Published by Elsevier Science Ltd.

Keywords: Fuel cells; Magnetic properties; Octahedral tilting; Perovskite

1. Introduction

Perovskite oxide $La_{1-x}Sr_xCoO_3$ is a mixed ionic and electronic conductor and has been widely investigated for use in various high-temperature electrochemical devices, such as in solid oxide fuel cells[1,2] or oxygen permeation membranes.[3] The compound with $x=0.5$ has the largest conductivity[4] and is rhombohedrally distorted.[5] To discuss the stability of the perovskite-type compounds ABO_3, Goldshmit introduced the tolerance factor (t) defined by

$$t = \frac{r_A + r_O}{\sqrt{2}(r_B + r_O)} \quad (1)$$

where r_A, r_B and r_O are the radii of the A and B cations and oxygen ion, respectively.[6] For tolerance factors less then unity, two types of distortion from the cubic structure, the rhombohedral and the orthorhombic structure, commonly occur.[7] $La_{0.5}Sr_{0.5}CoO_3$ is a rhombohedral perovskite with $t=0.9736$. The properties of $La_{0.5}Ba_{0.5}CoO_3$ are similar to that of $La_{0.5}Sr_{0.5}CoO_3$ in many aspects. It is found that the crystal structure of $La_{0.5}Ba_{0.5}CoO_3$ is cubic.[8] The radii of Ba^{2+} and Sr^{2+} is 1.74 Å and 1.54 Å, respectively. When Ba substituted $La_{0.5}Sr_{0.5}CoO_3$ is formed, its tolerance factor becomes closer to unity. Therefore it is expected that the distortion of the solid solutions becomes smaller with the Ba substitution. Sathe et al.[9] carried out neutron diffraction studies on $La_{0.5}Sr_{0.5}CoO_3$. Although extensively studied, there is scarce published information about the structural, electrical and magnetic properties of Ba substituted $La_{0.5}Sr_{0.5}CoO_3$. In this paper, we have studied the electrical and magnetic properties of $La_{0.5}Sr_{0.25}Ba_{0.25}CoO_3$ and compared with those of $La_{0.5}Sr_{0.5}CoO_3$. We will present a detailed determination of the structure of $La_{0.5}Sr_{0.5}CoO_3$ and $La_{0.5}Sr_{0.25}Ba_{0.25}CoO_3$ by X-ray and neutron powder diffraction.

2. Experimental

The samples were prepared using standard ceramic technique. The starting materials were La_2O_3 (99.9%),

* Corresponding author. Tel.: +82-42-869-4253; fax: +82-42-869-4273.

E-mail address: joyride@cais.kaist.ac.kr (H.J. Kim).

0955-2219/01/$ - see front matter © 2001 Published by Elsevier Science Ltd.
PII: S0955-2219(01)00113-3

$SrCO_3$ (99.9%), $BaCO_3$ (99.9%) and CoO (99%). They were ground, pressed into pellets and fired in air at 1000°C for 12 h. This process was repeated three times. The samples were finally sintered at 1250°C for 24 h. The resistivity of the samples was measured using the standard four-probe technique. The dc magnetic susceptibilities were measured with a SQUID (Quantum Design, MPMS model) via zero field cooling and field cooling processes in the temperature range 5–300 K. The applied external magnetic field was 50 Oe. Powder X-ray diffraction patterns were measured at room temperature ($2\theta = 20-80°$) on a Rigaku Rotaflex diffractometer, using CuK_α radiation ($\lambda = 1.5406$ Å) equipped with a graphite monochromator. The neutron powder diffraction was collected at room temperature on a high-resolution powder diffractometer (HRPD) ($\lambda = 1.8339$ Å, $2\theta = 20 \sim 140°$) at the Hanaro reactor, Korea Energy Research Institute. Structure refinements were carried out by fitting the combined X-ray and neutron profiles with the program Fullprof which adopts the Rietveld method.[10] The lattice parameters, fractional coordinates, and displacement parameters of the cations were determined by the Rietveld refinement of X-ray profile. The fractional coordinates and displacement parameters of the oxygen atoms were determined from the neutron profile.

3. Results

3.1. Electrical and magnetic properties

The resistivity of $La_{0.5}Sr_{0.5}CoO_3$ sample is 150 μΩcm at room temperature. The resistivity of $La_{0.5}Sr_{0.25}Ba_{0.25}CoO_3$ is increased with the Ba substitution to 730 μΩcm.

Fig. 1 shows the temperature dependence of dc magnetization for $La_{0.5}Sr_{0.5-x}Ba_xCoO_3$ ($x = 0.0$ and 0.25) in the zero field cooled and field cooled conditions. It is seen that the large difference between field cooled M_{FC} and zero field cooled M_{ZFC} exists below Curie temperature T_c (≈225 K) for both specimens and the Curie temperature T_c decreases by Ba^{2+} substitution. According to the phase diagram suggested for $La_{1-x}Sr_xCoO_3$ on the basis of magnetization measurements, $La_{0.5}Sr_{0.5}CoO_3$ belongs to the cluster glass phase.[11] The absence of a true long range order is manifested by the large difference between M_{FC} and M_{ZFC} below T_c.[12] Therefore, it is expected that the difference between M_{FC} and M_{ZFC} is related the cluster glass phase, indicating the presence of the short range ferromagnetic order within a cluster.

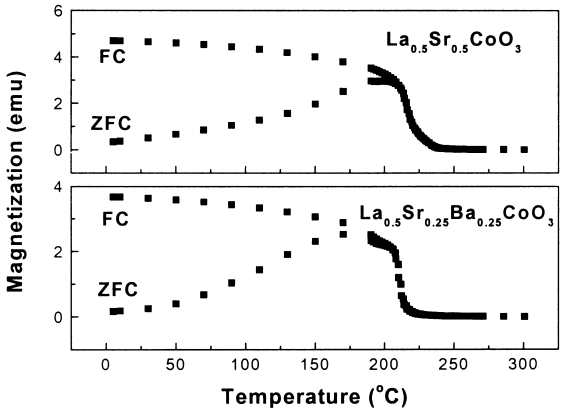

Fig. 1. Temperature dependence of magnetization of $La_{0.5}Sr_{0.5-x}Ba_xCoO_3$ ($x = 0.0$ and 0.25).

3.2. Structural studies

Fig. 2 shows the X-ray diffraction profiles of $La_{0.5}Sr_{0.5-x}Ba_xCoO_3$ ($x = 0.0$ and 0.25) at room temperature. All the $La_{0.5}Sr_{0.5-x}Ba_xCoO_3$ ($x = 0.0$ and 0.25) samples are of single perovskite phase without pyrochlore phase. Neutron diffraction measurements were performed for $La_{0.5}Sr_{0.5-x}Ba_xCoO_3$ ($x = 0.0$ and 0.25) to determine the precise crystal structure at room temperature. They are shown in Fig. 3. In addition to the fundamental reflection lines of a typical simple perovskite, extra diffraction lines are also observed in the

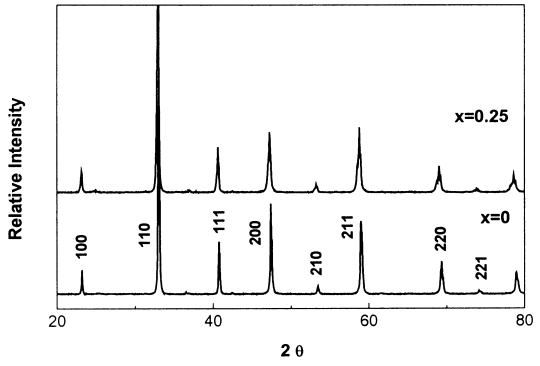

Fig. 2. The room temperature X-ray diffraction profiles of $La_{0.5}Sr_{0.5-x}Ba_xCoO_3$ ($x = 0.0$ and 0.25). Residual lines may be identified by the indices based on a simple cubic cell.

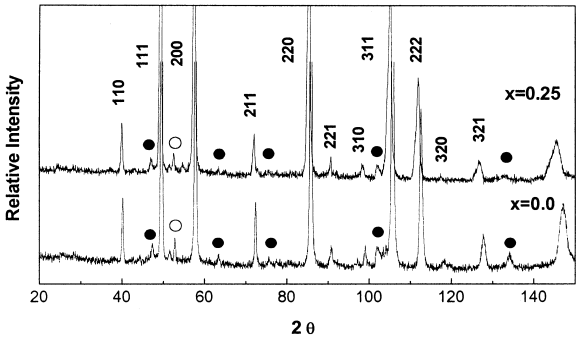

Fig. 3. The room temperature neutron diffraction profile of $La_{0.5}Sr_{0.5-x}Ba_xCoO_3$ ($x = 0.0$ and 0.25). Open and filled circles represent Co-rich peak and extra reflection lines, respectively.

neutron profiles. It is expected that these extra diffraction lines imply some degree of deviation from the cubic symmetry. Under the topological and geometrical constraints, three structural degrees of freedom of distortion from the ideal cubic perovskite structure are considered to be possible:[13] (i) displacements of the cations A and B from the centers of the polyhedra, (ii) distortion of the anion octahedra and (iii) tilting of the BO_6 octahedra. Neutron diffraction provides more information about oxygen octahedra tilting than X-ray because the neutron scattering power of O is comparable to that of the cations. With the low atomic number, the oxygen contribution to the diffraction lines is negligible in X-ray diffraction while its contribution is clearly recognizable in neutron diffraction. The pronounced presence of superlattice lines in the neutron diffraction profile rather than in the X-ray diffraction indicates that they are attributed to the change in oxygen arrangement in the crystal, either due to the distortion of the octahedra or more so to the tilting of the BO_6 octahedra. We analyzed our data on the assumption that these superlattice reflections are the result of the BO_6 octahedra tilting. The open circle in Fig. 3 indicates the peak which is related to a Co-rich phase.[14] Filled circles in Fig. 3 denote the extra reflection lines which are defined by the odd-odd-odd indices such as (3/2 1/2 1/2), (3/2 3/2 1/2) and (3/2 3/2 3/2). These results mean that the antiphase (a^-) octahedra tilting is along all the Cartesian coordinate axes ($a^-a^-a^-$) by Glazer's notation.[15] According to Woodward, the rhombohedral space group $R\bar{3}c$ results when an $a^-a^-a^-$ type tilt is present. Our refinements were performed in this space group. The observed and the fitted patterns are shown in Fig. 4. The final crystallographic data are listed in Table 1. The refined lattice parameters of $La_{0.5}Sr_{0.5}CoO_3$ are $a=b=$ 5.41795(2) Å, $c=13.25965(7)$ Å. When the solid solution $La_{0.5}Sr_{0.25}Ba_{0.25}CoO_3$ is formed, the length of a- and c-axis [$a=b=$ 5.45527(2) Å, $c=13.35097(6)$ Å] is larger than that of $La_{0.5}Sr_{0.5}CoO_3$. We find that the space group $R\bar{3}c$ defines the room-temperature crystal structure of $La_{0.5}Sr_{0.5-x}Ba_xCoO_3$ ($x=0.0$ and 0.25) well. Fig. 5 shows schematic views of the room-temperature structure of $La_{0.5}Sr_{0.5-x}Ba_xCoO_3$ ($x=0.0$ and 0.25), based on Table 1. We can clearly distinguish between the upper side and the lower side CoO_6 octahedra tilting, as shown in Fig. 5(a)–(c) for $x=0.0$. The pictures indicate $a^-a^-a^-$ tilting take place. The reason why the oxygen octahedra tilting occurs originates from the size difference between the A- and octahedral sites. Since the Sr space volume of the A-site in Sr substituted $LaCoO_3$ is smaller than that of the oxygen octahedral site, the perovskite cubic structure becomes unstable. To compensate for the instability, oxygen octahedra tilting takes place. As a consequence, the size difference between the A- and octahedral sites decreases. Ba^{2+} (1.74 Å ionic radius) substitution for Sr^{2+} (1.54 Å) diminishes the mismatch in size between the A-site and octahedral space volumes. Therefore we suppose that the degree of tilting decreases with increasing Ba^{2+} substitution. As shown Fig. 6(a) and (b), the octahedra tilting becomes smaller on Ba^{2+} substitution. The

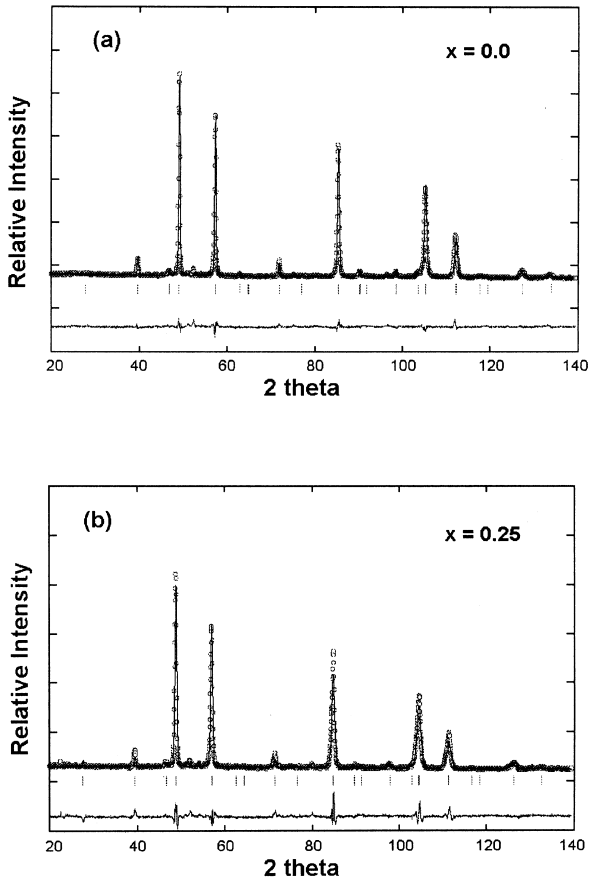

Fig. 4. Powder neutron diffraction patterns (circles: observed; line: calculated) of $La_{0.5}Sr_{0.5-x}Ba_xCoO_3$ ($x=0.0$ and 0.25) with the difference profiles shown below.

Table 1
Crystallographic data for $La_{0.5}Sr_{0.5}CoO_3$ and $La_{0.5}Sr_{0.25}Ba_{0.25}CoO_3$ at room temperature from powder neutron diffraction profiles

Atom	x	y	z	B
$x=0$	space group	$R\bar{3}$ c (No. 167)		
$a=b=5.41795(2)$ Å		$c=13.25965(7)$		
$R_{wp}=5.84$ (neutron)		$R_{Bragg}=3.71$	(neutron)	
$R_{wp}=14.6$ (X-ray)		$R_{Bragg}=2.85$	(X-ray)	
La, Sr	0.0	0.0	0.25	0.4323(4)
Co	0.0	0.0	0.0	0.3783(4)
O	0.4814(3)	0.0	0.25	0.9657(6)
$x=0.25$	space group	$R\bar{3}c$ (No. 167)		
$a=b=$ 5.45527(2)Å		$c=13.35097(6)$		
$R_{wp}=7.59$ (neutron)		$R_{Bragg}=4.70$	(neutron)	
$R_{wp}=18.3$	(X-ray)	$R_{Bragg}=8.81$	(X-ray)	
La, Sr	0.0	0.0	0.25	0.4323(3)
Co	0.0	0.0	0.0	0.3783(3)
O	0.4921(3)	0.0	0.25	0.9657(6)

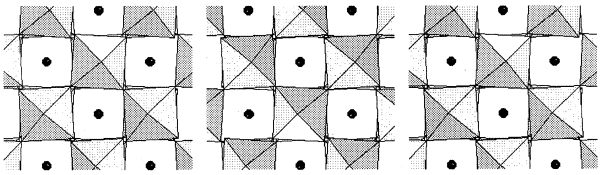

Fig. 5. Schematic projections of the $La_{0.5}Sr_{0.5}CoO_3$ crystal structure on the plane normal to the octahedral along three Cartesian coordinate axes: (a), (b) and (c). The $a^-a^-a^-$ tilting characteristic is clearly seen.

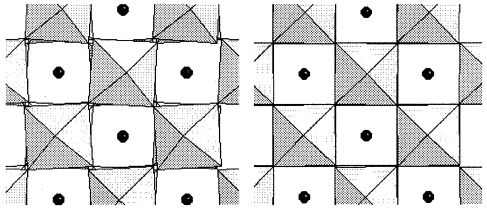

Fig. 6. Schematic projections of the crystal structures of (a) $La_{0.5}Sr_{0.5}CoO_3$ and (b) $La_{0.5}Sr_{0.25}Ba_{0.25}CoO_3$ along one of the three Cartesian coordinate axes. We can see the almost cubic symmetry of $La_{0.5}Sr_{0.25}Ba_{0.25}CoO_3$.

Co–O–Co bond angles reach almost 180° in $La_{0.5}Sr_{0.25}Ba_{0.25}CoO_3$ (173.976°; $x=0.0$ and 177.482°; $x=0.25$). This result coincides with the assumption that the distortion of $La_{0.5}Sr_{0.25}Ba_{0.25}CoO_3$ may be smaller than that of $La_{0.5}Sr_{0.5}CoO_3$.

4. Conclusions

The conductivity of $La_{0.5}Sr_{0.25}Ba_{0.25}CoO_3$ is smaller than that of $La_{0.5}Sr_{0.5}CoO_3$. In field cooled and zero field cooled magnetization curves, both $La_{0.5}Sr_{0.5}CoO_3$ and $La_{0.5}Sr_{0.25}Ba_{0.25}CoO_3$ show large difference between M_{FC} and M_{ZFC} which is a manifestation of cluster-glass like behavior. The crystal structure of $La_{0.5}Sr_{0.5-x}Ba_xCoO_3$ ($x=0.0$ and 0.25) at room temperature is rhombohedral with space group $R\bar{3}c$ showing superlattice diffraction lines in the neutron diffraction profiles, in addition to the fundamental reflection lines of a typical simple perovskite. This means that the $a^-a^-a^-$ type oxygen octahedra tilting is present. It is clearly seen that the oxygen octahedra tilting decreases by Ba^{2+} substitution.

Acknowledgements

This work was supported by nano-projects (No. 99-J-MF-01-B-04) sponsored by Korea Research Institute of Standards and Science. The Authors deeply appreciate the support.

References

1. Minh, N. Q., Ceramic fuel cells. *J. Am. Ceram. Soc.*, 1993, **76**(3), 563–588.
2. Petrov, A. N., Kononchuk, O. F., Andreev, A. V., Cherepanov, V. A. and Kofastd, P., Crystal structure, electrical and magnetic properties of $La_{1-x}Sr_xCoO_{3-y}$. *Solid State Ionics*, 1995, **80**, 189–199.
3. Van Hassel, B. A., Kawada, T., Sakai, N., Yokokawa, H., Dokiya, M. and Bouwmeester, H. J. M., Oxygen permeation modeling of $La_{1-y}Ca_yCrO_{3-\delta}$. *Solid State Ionics*, 1993, **66**, 41–47.
4. Jonker, G. H. and Van Santen, J. H., *Physica*, 1953, **120**, 19.
5. Mineshige, A., Inaba, M., Yao, T. and Ogumi, Z., Crystal structure and metal-insulator transition of $La_{1-x}Sr_xCoO_3$. *J. Solid State Chem.*, 1996, **121**, 423–429.
6. Woodward, P. M., Octahedral tilting in perovskites. ‡U. Structure stabilizing forces. *Acta Crystall*, 1997, **B53**, 44–66.
7. Tezuka, K., Hinatsu, Y., Nakamura, A. and Inami, T., Magnetic and neutron diffraction study on perovskites $La_{1-x}Sr_xCrO_3$. *J. Solid State Chem.*, 1998, **141**, 404–410.
8. Troyanchuk, I. O., Kasper, N. V. and Khalyavin, D. D., Magnetic and structural phase transitions in some orthocobaltites doped by Ba or Sr ions. *J. Phys.: Condens. Matter.*, 1998, **10**, 6381–6389.
9. Sathe, V. G., Pimpale, A. V., Siruguri, V. and Paranjpe, S. K., Neutron diffraction studies of perovskite-type compounds $La_{1-x}Sr_xCoO_3$ ($x=0.1$, 0.2, 0.3, 0.4, 0.5). *J. Phys.: Condens. Matter.*, 1996, **8**, 3889–3896.
10. Rodriguez-Carvajal, J., Recent advances in magnetic structure determination by neutron powder diffraction. *Physica B*, 1993, **192**, 55–69.
11. Itoh, M., Natori, I., Kubota, S. and Motoya, K., Spin-glass behavior and magnetic phase diagram of $La_{1-x}Sr_xCoO_3$. *J. Phys. Soc. Jpn.*, 1994, **63**, 1486–1493.
12. Mukherjee, S., Ranganathan, R., Anilkumar, P. S. and Joy, P. A., Static and dynamic reponse of cluster glass in $La_{1-x}Sr_xCoO_3$. *Phys. Rev.*, 1996, **B54**, 9267–9273.
13. Woodward, P. M., Octahedral tilting in perovskites. I Geometrical considerations. *Acta Crystall.*, 1997, **B53**, 32–43.
14. Morin, F., Trudel, G. and Denos, Y., The phase stability of $La_{0.5}Ca_{0.5}CoO_{3-\delta}$. *Solid State Ionics*, 1997, **96**, 129–139.
15. Glazer, A. M., The classification of tilted octahedral in perovskites. *Acta Crystall.*, 1972, **B28**, 3384–3392.